



Novel VEGFR-2 kinase inhibitors identified by the back-to-front approach

Kingkan Sanphanya^a, Suvara K. Wattanapitayakul^b, Suwadee Phowichit^b, Valery V. Fokin^c, Opa Vajragupta^{a,*}

^a Excellent Center for Innovation in Drug Design and Discovery, Faculty of Pharmacy, Mahidol University, 447 Sri-Ayudya Rd, Bangkok 10400, Thailand

^b Department of Pharmacology, Faculty of Medicine, Srinakharinwirot University, 114 Sukhumvit 23, Bangkok 10110, Thailand

^c Department of Chemistry, The Scripps Research Institute, 10550 North Torrey Pines Rd, La Jolla, CA 92037, USA

ARTICLE INFO

Article history:

Received 9 November 2012

Revised 10 February 2013

Accepted 12 March 2013

Available online 20 March 2013

Keywords:

VEGFR-2

KDR

VEGFR-2 inhibitor

Molecular modeling

Antiangiogenesis

1,4-Disubstituted 1,2,3-triazoles

CuAAC reaction

ABSTRACT

We report a novel VEGFR-2 inhibitor, developed by the back-to-front approach. Docking experiments indicated that the 3-chloromethylphenylurea motif of the lead compound occupied the back pocket of VEGFR-2 kinase. An attempt was made to enhance the binding affinity of **1** by expanding the structure to access the front pocket using a triazole linker. A library of 1,4-(disubstituted)-1H-1,2,3-triazoles were screened in silico, and one compound (**VH02**) was identified with an IC₅₀ against VEGFR-2 of 0.56 μM. **VH02** showed antiangiogenic effects, inhibiting tube formation in HUVEC cells (EA.hy926) at 0.3 μM, 13 times lower than its cytotoxic dose. These enzymatic and cellular activities suggest that **VH02** has potential as a lead for further optimization.

© 2013 Elsevier Ltd. All rights reserved.

Receptor tyrosine kinases (RTKs) are a class of protein tyrosine kinase that regulate inter- and intracellular communications by signal transduction. These proteins play a major role in the regulation of cell growth, proliferation, differentiation, survival and metabolism.^{3,4} Among RTKs, vascular endothelial growth factor receptor-2 (VEGFR-2) is a major target in suppressing cancer growth and metastasis because of its vital role in the regulation of angiogenesis.^{5–8}

Tyrosine kinase inhibitors can be classified into two main types according to binding pose. Type I inhibitors bind specifically to the adenine-binding or ATP site of kinases in the active form, and type II inhibitors bind to the ATP site and an additional hydrophobic back pocket, an allosteric site found in the inactive form of the kinase. Different conformations are observed in the active and inactive states of tyrosine kinases at the beginning of the activation loop, which is composed of the highly conserved triad Asp-Phe-Gly (DFG). In the active state the kinase adopts a 'DFG-in' conformation, whereas in the inactive state it adopts a 'DFG-out' conformation (Fig. 1). Type II kinase inhibitors are generally more selective than type I inhibitors.^{9–14} Thus, the binding site normally targeted in the structure-based drug design of small-molecule

kinase inhibitors is composed of a front ATP-binding pocket and a hydrophobic back pocket formed by the DFG-out conformation.¹⁵ In the front pocket, the two key amino acid residues that participate in H-bond interactions with the adenine ring of ATP are Glu917 and Cys919, which are located in the hinge area of the binding site. The two key amino acids in the back pocket that participate in H-bond interactions are Glu885, locating in the αC-helix, and Asp1046, a part of the DFG-motif in the activation loop. Apparently, most VEGFR-2 inhibitors form hydrogen bonds with these key amino acid residues.^{16–18}

The 'back-to-front' approach—the design of type II kinase inhibitors starting from the back pocket and expanding the core structure towards the front pocket—is one strategy used in drug development targeting protein kinases. This approach was successful in finding lead p38α kinase inhibitors,¹⁹ cFMS kinase inhibitors²⁰ and VEGFR-2 inhibitors.²¹

We previously reported lead compound (**1**), 1-((3-chloromethyl) phenyl)-3-(2-propynyl)urea, which inhibits EGFR. This compound did not inhibit VEGFR-2 at the screening concentration (1 μM).²² In this work, we have attempted to develop a novel class of VEGFR-2 inhibitors using **1** as the core structure, because docking simulations of **1** in the active site of VEGFR-2 kinase revealed that this compound only occupied the allosteric site (Fig. 2). Both urea HN moieties of **1** acted as hydrogen bond donors (HBD).

* Corresponding author. Tel./fax: +66 26 448 695.

E-mail address: pyovj@mahidol.ac.th (O. Vajragupta).

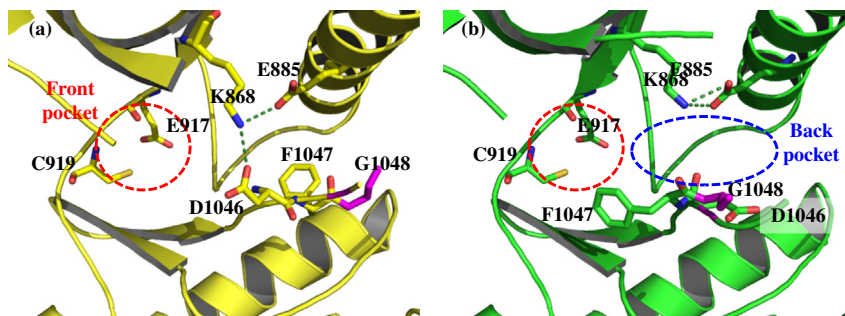


Figure 1. The binding site in the VEGFR-2 kinase domain, with key residues participating in H-bonds highlighted (a) DFG-in conformation (PDB code: 3B8R)¹ showing the ATP-binding site (red circle) and two salt bridges from Lys868 (green dotted lines); (b) DFG-out conformation (PDB code: 3EWH)², showing the allosteric pocket (blue circle) behind the ATP site.

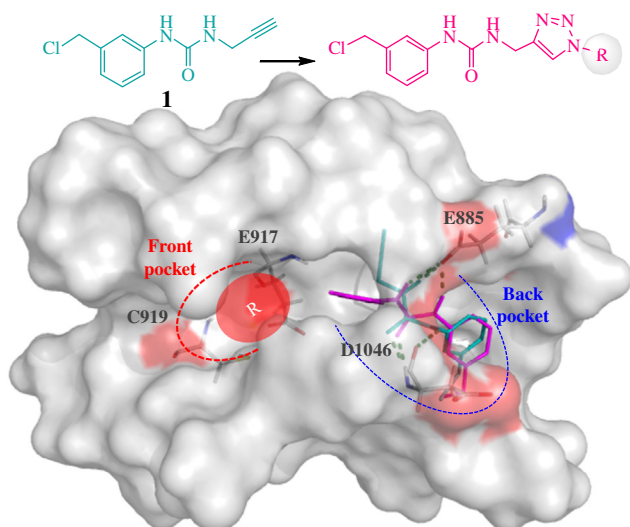


Figure 2. 'Back to front' design strategy. Compound **1** (blue) as starting motif buried in back pocket. Substituted group (R) on triazole to occupy the front pocket.

One urea *HN* interacted with the backbone carbonyl of Asp1046, while the other interacted with that of Glu885. The urea carbonyl moiety of **1** also acted as a hydrogen bond acceptor (HBA) by interacting with the backbone NH-amide of Asp1046. The 3-chloromethylphenyl substructure was buried in the hydrophobic back pocket and directed the terminal alkyne moiety to the front pocket. Based on this data, **1** was chosen as the starting fragment in the development of novel VEGFR-2 kinase inhibitors.

To design novel VEGFR-2 kinase inhibitors by the back-to-front approach, we started by anchoring **1** in the hydrophobic back pocket. Lead **1** possesses a terminal alkyne, a potential building block for the preparation of 1,4-disubstituted-1*H*-1,2,3-triazoles, by copper-catalyzed azide-alkyne cycloaddition (CuAAC). Therefore a virtual library of [1-(substituted)-1*H*-[1,2,3]-triazol-4-yl]-methyl-3-[3'-(chloromethyl)phenyl]ureas was designed by adding a substituent (R) to the triazole linker. The design strategy is to extend the structure of phenylurea **1** with various substituents (R) that fit the front pocket closely and thus increase the binding affinity.

This library of 90 [1-(substituted)-1*H*-[1,2,3]-triazol-4-yl]-methyl-3-[3'-(chloromethyl)phenyl]ureas was screened virtually by docking experiments. Details of VEGFR-2 template preparation and validation were described previously.²² Briefly, the protein target was constructed from the crystal structure of inactive VEGFR-2 (DFG-out conformation) in complex with K11 (PDB ID: 3EWH).² The two missing loops were reconstructed (Super Looper Web

Server²³) before minimizing the energy (AMBER94 force field in MOE—Molecular Operating Environment—Chemical Computing Group, Montreal, Quebec, Canada). Nonpolar hydrogens from a new template (3EWHOK) were merged before adding Gasteiger Huckel charges (AutoDockTools-1.5.2^{24,25}). Then, atom types were assigned, and a grid representation of 3EWHOK was prepared (AutoGrid4²⁵). The 3EWHOK template was validated by docking (AutoDock 4.2, TSRI)²⁵ six active inhibitors (K11, AAX, GIG, LIF, 887 and 900, from PDB IDs 3EWH,² 1Y6B,²⁶ 2OH4,²⁷ 1YWN,²⁸ 3B8R,¹ and 3B8Q,¹ respectively). All docked poses were the same as in the corresponding crystal structures, with RMSD less than 2 Å. These results indicated that 3EWHOK was a good VEGFR-2 model for *in silico* experiments.

Virtual hits were selected by analysis of the docking results (Fig. 3). The criteria for selecting hits were the free energy of binding (ΔG), hydrogen bonding interaction with key amino acid residues and docked conformation by visual inspection. In addition to two hydrogen bonds between core urea *NH* groups and key residues in the back pocket (Asp1046 or Glu885), the virtual hits were required to form extra hydrogen bonds with at least one of the key residues in the ATP-binding pocket (either Glu917 or Cys919). The docking results for eleven virtual hits are summarized in Table 1.

The hits (**VH01–VH11**) showed notably lower binding energy comparing with compound **1** (Table 1). As anticipated, all compounds occupied both back and front pockets in a similar manner, with the phenylurea moiety buried in the hydrophobic back pocket

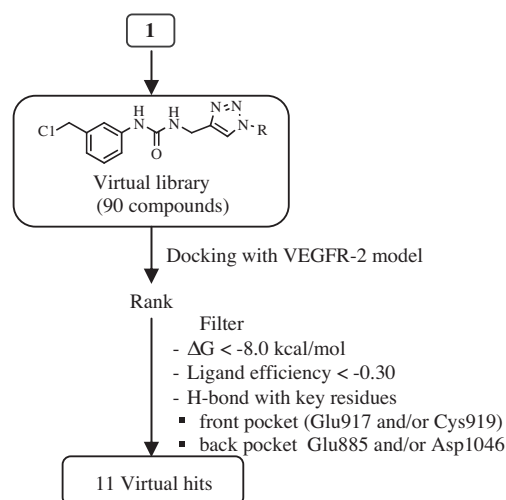


Figure 3. *In silico* experiments to identify hits.

Table 1
Selected virtual hits for synthesis^a

Compd	R	Free energy of binding (ΔG , kcal/mol)	H-bonding with key residues
VH01		-9.60	Glu885, Glu885, Cys919, Asp1046
VH02		-9.96	Glu917, Cys919, Asp1046
VH03		-10.13	Glu885, Cys919, Asp1046
VH04		-10.13	Glu885, Glu885, Cys919, Asp1046
VH05		-10.95	Glu885, Glu885, Cys919, Asp1046
VH06		-10.40	Glu885, Glu885, Cys919, Asp1046
VH07		-10.48	Glu885, Cys919
VH08		-10.65	Glu885, Glu885, Cys919, Asp1046
VH09		-10.42	Glu885, Glu885, Cys919, Asp1046
VH10		-10.04	Cys919, Asp1046
VH11		-10.41	Glu885, Glu885, Cys919

^a Docking result for **1**: free energy of binding was -6.47 kcal/mol; H-bonding residues were Glu885, Asp1046 and Asp1046.

and the substituent (R) extended to fit the front pocket. The overlay model of **VH02** and sorafenib was illustrated in [Figure 4](#).

The selected virtual hits were synthesized for biological testing. The general synthesis procedure for 11 hits was the CuAAC reaction ([Scheme 1](#)). Briefly, **1** and one equivalent of the corresponding azide building block were added into a 25 mL round-bottom flask and suspended in *t*-BuOH/EtOH/H₂O (2:1:1). Then 5 mol % of CuSO₄ and 20 mol % of sodium ascorbate were added to the stirred reaction mixture and heated at 60 °C for 1–2 h. The precipitates formed were washed several times with cool diethyl ether before filtering. Pure products were collected as off-white to yellow powders. In some

cases, products were purified by column chromatography on silica gel using 5–7% MeOH in dichloromethane as eluent (unoptimized yields were 12–94%). All of the synthesized compounds were characterized by IR, NMR and by high-resolution mass spectroscopy. The assigned structures of all synthesized compounds were in agreement with the designed structures (see [Supplementary data](#)).

All synthesized compounds were then screened for kinase inhibition at 1 μ M against three RTKs: VEGFR-2, EGFR and PDGFR- β ([Fig. 5](#)). The ability of compounds to inhibit phosphorylation of a biotinylated polypeptide substrate were measured by a previously described protocol.²²

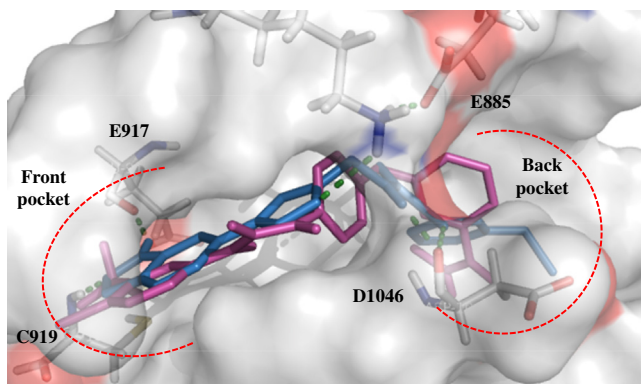
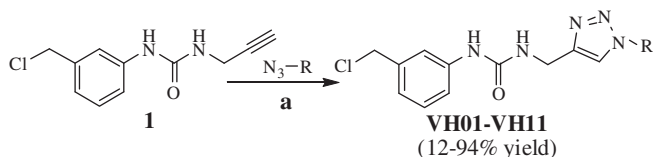


Figure 4. Overlay model of **VH02** (blue) and sorafenib (magenta) bound to the VEGFR-2 kinase domain (PDB code: 3EWHOK),² showing 4 H-bonds in front and back pockets (green dotted lines).



Scheme 1. Synthesis of selected virtual hits by CuAAC reaction. (a) 5 mol % CuSO₄, 20 mol % sodium ascorbate, *t*-BuOH/EtOH/H₂O (1:1:2), 60 °C, 1–2 h.

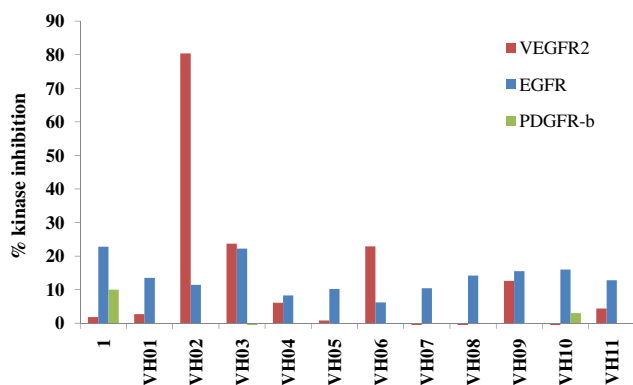


Figure 5. Screening result at 1 μ M of hit compounds against three tyrosine kinases.

At 1 μ M **VH02**, the 6-indazolyl triazole derivative was the only compound that noticeably inhibited phosphorylation of VEGFR-2. The IC₅₀ of **VH02** against VEGFR-2 was 0.56 μ M. Modest inhibition of EGFR was observed for all synthesized compounds. Only the 5-indazolyl triazole (**VH03**) exhibited activity against EGFR comparable to **1**, while the other extended triazoles exhibited diminished potency against this tyrosine kinase. Inhibition of PDGFR- β was not observed for any compound. Though its inhibition against VEGFR kinase was not as potent as sorafenib (IC₅₀ = 90 nM)^{29,30}, **VH02** from in silico screening was considered as the most promising lead VEGFR-2 inhibitor.

The kinase inhibitory activity of **VH02** against VEGFR-2 can be explained by its binding mode from molecular modeling. Though the binding energy of **VH02** was not significantly different from other hits, the H-bonding interaction between **VH02** and key residues in the front pocket of VEGFR-2 kinase was different from the others. The 6-indazolyl substructure of **VH02** formed two hydrogen bond interactions with the key residues, Glu917 and Cys919, in the front pocket of VEGFR-2 kinase, while the corresponding triazole substructures (R) of other hits formed only one H-bond with

Cys919, a key residue in the front pocket. The extra H-bond between **VH02** and key residues observed in the front pocket of VEGFR-2 help to explain the activity of **VH02** over other hits. In total, **VH02** formed 5 H-bonds with key amino acids in the binding site of VEGFR-2 kinase. The indazolyl NH acted as HBD, forming one hydrogen bond with the backbone carbonyl of Glu917, while the N-2 indazole acted as HBA, forming a H-bond with the backbone NH of Cys919. The aromatic part of the indazole ring interacted with a hydrophobic region within the front pocket. This area composed of the side chains of Leu840, Val848, Ala866, Lys868, Glu917 Phe918 and Gly922. The triazole linker of **VH02** participated in one H-bond, using the N-2 triazole as HBA to interact with the side chain NH of Lys868. The urea moiety formed two hydrogen bonds with key residues in the back pocket of VEGFR-2 kinase. Both urea NH groups formed H-bonds with the same backbone carbonyl of Asp1046. The substituted phenyl motif of **VH02** was buried in the hydrophobic part of the back pocket and interacted with the side chains of Ile888, Ile892, Val898, Val899, Leu1019, His1026, Ile1044, Cys1045 and Phe1047. The hydrophobic interactions both in the front and allosteric pocket moderated the binding affinity and selectivity by stabilizing the proper conformation of the compound in the binding site of VEGFR-2 kinase.

The docking of **VH02** and sorafenib against VEGFR2 revealed that **VH02** aligned in the binding site of VEGFR-2 in the similar way to that of sorafenib with % members in the highest cluster of 74% and 81% for **VH02** and sorafenib, respectively. Polar substructures of both **VH02** and sorafenib occupied the front ATP-binding pocket and less polar substructures of both compounds buried in the hydrophobic back pocket (Fig. 4). It was found that **VH02** bound with VEGFR-2 with higher free binding energy (−9.96 kcal/mol vs −14.92 kcal/mol) and formed less numbers of H-bond interaction with key residues in both pockets (5 H-bonds vs 3 H-bonds) which may be the main reason for less potency of **VH02** as VEGFR-2 inhibitor.

The docking between **VH02** and the active site of EGFR kinase was performed and compared with erlotinib, the prototype of EGFR inhibitor; the docking result of **VH02** against EGFR answered the observed poor activity of this compound against EGFR. Instead of anchoring in the hydrophobic back pocket as expected, the 1-((3-chloromethyl)phenyl)-3-urea substructure of **VH02** pointed out to the water accessible cavity of EGFR binding site while the indazole–triazole substructure aligned in the back hydrophobic cavity (Fig. 6). No hydrogen bond interaction was observed between **VH02** and the backbone carboxylate of conserved Met769, a hinge residue in the ATP site, while erlotinib established a hydrogen

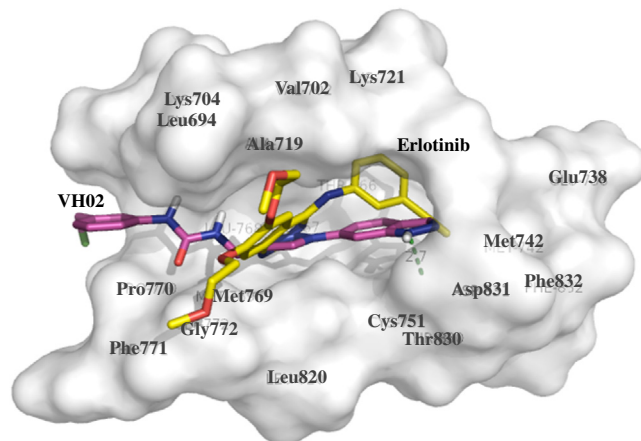


Figure 6. The overlay between docked-pose of **VH02** (magenta) and erlotinib (yellow) in the active site of EGFR (PDB code: 1M17).

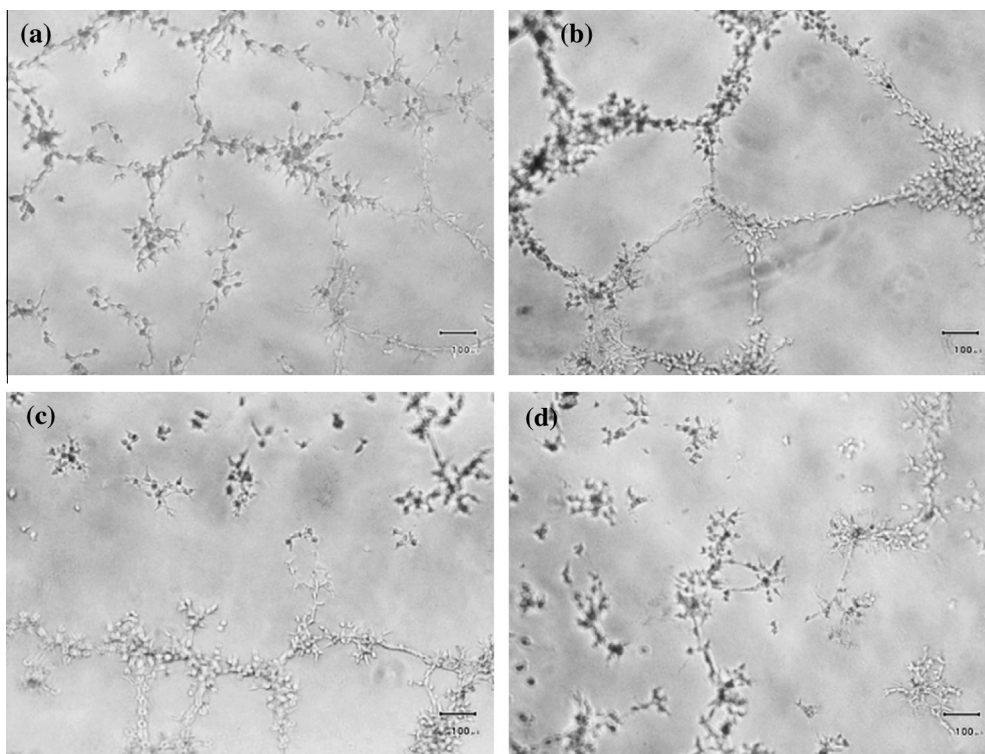


Figure 7. Effect of **VH02** on VEGF-stimulated tube formation at 10× magnification. (a) 0.1% DMSO; (b) control with VEGF 25 ng/mL (c) and (d) treatment with **VH02** 0.3 and 1.0 μM, respectively.

bond with this key amino acid residue (see [Supplementary Data](#)). In addition, the possibility of **VH02** to conform in good binding pose is low, % conformations in the highest cluster was significantly lower (45% vs 100%) despite of better affinity than erlotinib (−9.10 kcal/mol vs −7.48 kcal/mol).

VH02 was further evaluated for antiangiogenic effects. This compound was first screened for antiproliferative activity in immortal HUVECs (EA.hy926), which are frequently used for in vitro angiogenesis testing.^{31–33} The protocol for the antiproliferation assay was described previously.²²

The IC_{50} for **VH02** cytotoxicity against EA.hy926 was 4 μM which was comparable to that of sorafenib against HUVEC (IC_{50} = 4–5 μM)³⁴ despite of moderate inhibition against VEGFR2 kinase. The in vitro antiangiogenic effect of **VH02** was evaluated in a tube formation assay. The test was performed at a non-cytotoxic concentration to avoid false positives from the cytotoxicity. The results from the tube formation assay are shown in [Figure 7](#). **VH02** significantly inhibited tube formation at 0.3 μM, which was 13 times lower than its cytotoxic IC_{50} against EA.hy926. Additionally, the antiproliferative activity of **VH02** was investigated in four other cancer cell lines, including cervical cancer (HELA), human breast cancer (MCF-7), large cell lung cancer (H460) and hepatic carcinoma (HepG2). The results are summarized in [Table 2](#).

Table 2
Antiproliferative effect of **VH02** on cancer cells and EA.hy926

Type of cancer cells	IC_{50} (μM)
HELA	33
MCF-7	21
H460	71
HepG2	>100
EA.hy 926	4

The antiproliferative results indicated that **VH02** exhibited higher selectivity against EA.hy926 (representing vascular endothelial cells), with weak cytotoxicity against other cancer cells. Thus, this compound may be useful in the treatment of cancer, to avoid metastasis as well as to prolong time to recurrence with low toxicity.

In this study, molecular modeling protocol aided us in rapidly screening for potential hit compounds from a number of virtual compounds in the focus library. Back-to-front approach was proved to be an efficient strategy in drug design since the amino acid residues in the back pocket areas of each kinase were less conserved when comparing with those in the front pocket. The flipping of anchoring motif from the back pocket to front pocket significantly affected both selectivity and potency of the designed compound as observed in compound **1** and **VH02** against EGFR and VEGFR-2.

In conclusion, **VH02** was developed as a novel lead VEGFR-2 kinase inhibitor by a back-to-front approach, starting from a 3-(3'-chloromethylphenyl)urea fragment. A triazole ring was used as linker, due to its convenient synthesis by the CuAAC reaction. Enzyme inhibition and cellular activity indicated that this compound is an antiangiogenic agent that selectively inhibits VEGFR-2. Though it was not as potent as sorafenib, **VH02** can be considered a promising lead with a novel scaffold, suitable for further optimization.

Acknowledgments

This work was supported by the Royal Golden Jubilee Ph.D. Program (RGJ Grant No. PHD/0229/2547), Thailand Research Fund (TRF), The Office of the Higher Education Commission, Ministry of Education, Thailand (CHE-RG 2551) and the Office of the High Education Commission and Mahidol University under the National Research Universities Initiative.

Supplementary data

Supplementary data associated with this article can be found, in the online version, at <http://dx.doi.org/10.1016/j.bmcl.2013.03.042>.

References and notes

- Weiss, M. M.; Harmange, J.-C.; Polverino, A. J.; Bauer, D.; Berry, L.; Berry, V.; Borg, G.; Bready, J.; Chen, D.; Choquette, D.; Coxon, A.; DeMelfi, T.; Doerr, N.; Estrada, J.; Flynn, J.; Graceffa, R. F.; Harriman, S. P.; Kaufman, S.; La, D. S.; Long, A.; Neervannan, S.; Patel, V. F.; Potashman, M.; Regal, K.; Roveto, P. M.; Schrag, M. L.; Starnes, C.; Tasker, A.; Teffer, Y.; Whittington, D. A.; Zanon, R. *J. Med. Chem.* **2008**, *51*, 1668.
- Cee, V. J.; Cheng, A. C.; Romero, K.; Bellon, S.; Mohr, C.; Whittington, D. A.; Bak, A.; Bready, J.; Caenepeel, S.; Coxon, A.; Deak, H. L.; Fretland, J.; Gu, Y.; Hodous, B. L.; Huang, X.; Kim, J. L.; Lin, J.; Long, A. M.; Nguyen, H.; Olivieri, P. R.; Patel, V. F.; Wang, L.; Zhou, Y.; Hughes, P.; Geuns-Meyer, S. *Bioorg. Med. Chem. Lett.* **2009**, *19*, 424.
- Zwick, E.; Bange, J.; Ullrich, A. *Trends Mol. Med.* **2002**, *8*, 17.
- Culhane, J.; Li, E. *US Pharm.* **2008**, *33*, 3.
- Folkman, J. *Semin. Oncol.* **2002**, *29*, 15.
- Hoeben, A.; Landuyt, B.; Highley, M. S.; Wildiers, H.; Van Oosterom, A. T.; De Bruijn, E. A. *Pharmacol. Rev.* **2004**, *56*, 549.
- Schenone, S.; Bondavalli, F.; Botta, M. *Curr. Med. Chem.* **2007**, *14*, 2495.
- Holmes, K.; Roberts, O. L.; Thomas, A. M.; Cross, M. J. *Cell. Signal.* **2003**, *2007*, 19.
- Liu, Y.; Gray, N. S. *Nat. Chem. Biol.* **2006**, *2*, 358.
- Zhang, J.; Yang, P. L.; Gray, N. S. *Nat. Rev. Cancer* **2009**, *9*, 28.
- Okram, B.; Nagel, A.; Adrian, F. J.; Lee, C.; Ren, P.; Wang, X.; Sim, T.; Xie, Y.; Wang, X.; Xia, G.; Spraggon, G.; Warmuth, M.; Leu, Y.; Gray, N. S. *J. Chem. Biol.* **2006**, *13*, 779.
- Zuccotto, F.; Ardini, E.; Casale, E.; Angiolini, M. *J. Med. Chem.* **2010**, *53*, 2681.
- Kufareva, I.; Abagyan, R. J. *J. Med. Chem.* **2008**, *51*, 7921.
- Xie, Q.-Q.; Xie, H.-Z.; Ren, J.-X.; Li, L.-L.; Yang, S.-Y. *J. Mol. Graph. Model.* **2009**, *27*, 751.
- Schwartz, P. A.; Murray, B. W. *Bioorg. Chem.* **2011**, *39*, 192.
- Bauer, D.; Whittington, D. A.; Coxon, A.; Bready, J.; Harriman, S. P.; Patel, V. F.; Polverino, A.; Harmange, J.-C. *Bioorg. Med. Chem. Lett.* **2008**, *18*, 4844.
- Honda, T.; Nagahara, H.; Mogi, H.; Ban, M.; Aono, H. *Bioorg. Med. Chem. Lett.* **2011**, *21*, 1782.
- Sammond, D. M.; Nailor, K. E.; Veal, J. M.; Nolte, R. T.; Wang, L.; Knick, V. B.; Rudolph, S. K.; Truesdale, A. T.; Nartey, E. N.; Stafford, J. A.; Kumar, R.; Cheung, M. *Bioorg. Med. Chem. Lett.* **2005**, *15*, 3519.
- Regan, J.; Breitfelder, S.; Cirillo, P.; Gilmore, T.; Graham, A. G.; Hickey, E.; Klaus, B.; Madwed, J.; Moriak, M.; Moss, N.; Pargellis, C.; Pav, S.; Proto, A.; Swinamer, A.; Tong, L.; Torcellini, C. *J. Med. Chem.* **2002**, *45*, 2994.
- Baldwin, I.; Bamborough, P.; Haslam, C. G.; Hunjan, S. S.; Longstaff, T.; Mooney, C. J.; Patel, S.; Quinn, J.; Somers, D. O. *Bioorg. Med. Chem. Lett.* **2008**, *18*, 5285.
- Iwata, H.; Oki, H.; Okada, K.; Takagi, T.; Tawada, M.; Miyazaki, Y.; Imamura, S.; Hori, A.; Lawson, J. D.; Hixon, M. S.; Kimura, H.; Miki, H. *ACS Med. Chem. Lett.* **2012**, *3*, 342.
- Sanphanya, K.; Wattanapitayakul, S. K.; Prangsaengtong, O.; Jo, M.; Koizumi, K.; Shibahara, N.; Priprem, A.; Fokin, V. V.; Vajragupta, O. *Bioorg. Med. Chem. Lett.* **2012**, *22*, 3001.
- Hildebrand, P. W.; Goede, A.; Bauer, R. A.; Gruening, B.; Ismer, J.; Michalsky, E.; Preissner, R. *Nucleic Acids Res.* **2009**, *37*, W571.
- Forli, S.; Botta, M. *J. Chem. Inf. Model.* **2007**, *47*, 1481.
- Morris, G. M.; Huey, R.; Lindstrom, W.; Sanner, M. F.; Belew, R. K.; Goodsell, D. S.; Olson, A. J. *J. Comput. Chem.* **2009**, *30*, 2785.
- Harris, P. A.; Cheung, M.; Hunter, R. N.; Brown, M. L.; Veal, J. M.; Nolte, R. T.; Wang, L.; Liu, W.; Crosby, R. M.; Johnson, J. H.; Epperly, A. H.; Kumar, R.; Luttrell, D. K.; Stafford, J. A. *J. Med. Chem.* **2005**, *48*, 1610.
- Hasegawa, M.; Nishigaki, N.; Washio, Y.; Kano, K.; Harris, P. A.; Sato, H.; Mori, I.; West, R. I.; Shibahara, M.; Toyoda, H.; Wang, L.; Nolte, R. T.; Veal, J. M.; Cheung, M. *J. Med. Chem.* **2007**, *50*, 4453.
- Miyazaki, Y.; Matsunaga, S.; Tang, J.; Maeda, Y.; Nakano, M.; Philippe, R. J.; Shibahara, M.; Liu, W.; Sato, H.; Wang, L.; Nolte, R. T. *Bioorg. Med. Chem. Lett.* **2005**, *15*, 2203.
- Wilhelm, S. M.; Carter, C.; Tang, L.; Wilkie, D.; McNabola, A.; Rong, H.; Chen, C.; Zhang, X.; Vincent, P.; McHugh, M.; Cao, Y.; Shujath, J.; Gawlak, S.; Eveleigh, D.; Rowley, B.; Liu, L.; Adnane, L.; Lynch, M.; Auclair, D.; Taylor, I.; Gedrich, R.; Voznesensky, A.; Riedl, B.; Post, L. E.; Bollag, G.; Trail, P. A. *Cancer Res.* **2004**, *64*, 7099.
- Gollob, J. A.; Wilhelm, S.; Carter, C.; Kelley, S. L. *Semin. Oncol.* **2006**, *33*, 392.
- Wu, H.-T.; Lin, S.-h.; Chen, Y.-H. *J. Agric. Food Chem.* **2005**, *53*, 5164.
- Cong, M.; Xue-chun, L.; Yun, L.; Jian, C.; Bo, Y.; Yan, G.; Xian-feng, L.; Li, F. *Chin. Med. J.* **2012**, *125*, 1369.
- Jones, M. K.; Sarfeh, I. J.; Tarnawski, A. S. *Biochem. Biophys. Res. Commun.* **1998**, *249*, 118.
- Plastaras, J. P.; Kim, S.-H.; Liu, Y. Y.; Dicker, D. T.; Dorsey, J. F.; McDonough, J.; Cerniglia, G.; Rajendran, R. R.; Gupta, A.; Rustgi, A. K.; Diehl, J. A.; Smith, C. D.; Flaherty, K. T.; El-Deiry, W. S. *Cancer Res.* **2007**, *67*, 9443.